Electric fields imbue enzyme reactivity by aligning active site fragment orbitals

M.E. Eberhart,[*,†] Timothy R. Wilson,[†] T.E. Jones,[‡] and Anastassia N. Alexandrova[¶]

†Chemistry Department, Colorado School of Mines, 1500 Illinois Street, Golden, CO, USA

‡Theoretical Division, Los Alamos National Laboratory, Los Alamos, New Mexico 87545, USA

¶Department of Chemistry, and Biochemistry, University of California, Los Angeles, Los Angeles, California 90095, United States

E-mail: meberhar@mines.edu

Abstract

It is broadly recognized that intramolecular electric fields, produced by the protein scaffold and acting on the active site, facilitate enzymatic catalysis. This field effect can be described by several theoretical models, each of which is intuitive to varying degrees. In this contribution, we show that a fundamental effect of electric fields is to generate electrostatic potentials that facilitate the energetic alignment of reactant frontier orbitals. We apply this model to demystify the impact of electric fields on high-valent iron-oxo heme proteins: catalases, peroxidases, and peroxygenases/monooxygenases. Specifically, we show that this model easily accounts for the observed field-induced changes to the spin distribution within peroxidase active sites and explains the transition between epoxidation and hydroxylation pathways seen in Cytochrome P450 active site models. Thus, for the intuitive interpretation of the chemical effect of the field, the strategy involves analyzing the response of the orbitals of active site fragments, and their energetic alignment. We note that the energy difference between fragment orbitals involved in charge redistribution acts as a measure for the chemical hardness/softness of the reactive complex. This measure, and its sensitivity to electric fields, offers a single parameter model from which to quantitatively assess the effects of electric fields on reactivity and selectivity. Thus, the model provides an additional perspective to describe electrostatic preorganization and offer ways for its manipulation.

1

Introduction

Electric fields can profoundly affect chemical reactions, a fact that, while long utilized by nature in the creation of selective and efficient enzymes, was only recognized by scientists a little over fifty years ago.[1] This revelation ignited the imagination of researchers, envisioning a future where tailored electric fields could be used to synthesize new molecules and materials. Indeed, advancements in synthetic methods together with theoretical developments have propelled efforts to gain the insights and tools needed to manipulate electric fields to control the chemical behavior of surfaces, biomolecules, inorganic complexes, and microporous solids, to name but a few examples.[2–10] While the effects of electric fields have been discerned theoretically and experimentally, an overarching conceptual framework providing the predictive power to tailor electric fields is only now emerging.[11–14] Continued growth of this framework will necessarily draw from all the common tools in the chemist's toolkit. Toward this end, it is conceptually useful to distinguish three models to account for the field induced effects on chemical reactivity.

The foundation for the first of these models is provided by electron pushing formalisms and exemplified by the research by Aragonés et al.[2] They demonstrated that an appropriately oriented external electric field (OEEF) can enhance charge transfer and lower reaction barriers. In their study of a Diels-Alder reaction, model reactants were attached to an STM break junction, which was then supplied with an OEEF. The findings indicated that the reaction was facilitated by an alignment of the electric field that promoted electron flow from the dienophile to the diene. This hypothesis was further supported by broader research concluding that catalysis could generally be enhanced by orienting an electric field in the direction of electron reorganization during the reaction.[9]

The second model is an essential facet in Warshel's theory of electrostatic preorganization.[15,16] Warshel posited that the positioning of charged groups of the protein's extended structure is strategic to create local electric fields (LEFs) preorganized to reduce the energy of the transition state (TS), or in other words—align with the change of the electric dipole

moment upon TS crossing. Because the field is created by the charged amino acids of the protein backbone, the entropic penalty for the environmental reorganization during the reaction is avoided, and the barrier to the reaction is lowered. As an accompanying consequence, this same TS stabilizing field may, as in the Diels-Alder example above, promote the catalytic reaction's charge redistribution—further stabilizing the TS. Warshel and others (see Table 2 of Reference 16) have quantified these combined effects employing the empirical valence bond, EVB, method.[17]

The third model, commonly employed by the solid-state and electrochemistry communities, is firmly rooted in frontier orbital theory. This theory underscores the significance of the relative energies of the one-electron orbitals (or bands) in the reactants and the catalyst. A pertinent example is the work of Wasileski et al.,[18] who explored how the strength of the electric field affects the bonding of adsorbates to metal surfaces. They observed a correlation between the energy difference $E_f - E_a$ (E_f is the metal Fermi energy and E_a refers to the adsorbate valence energy levels) and various properties like the adsorbate's binding/adsorption energy. An applied electric field can adjust this energy difference, thereby modulating properties.

In the context of molecular systems, Model 3 dovetails with the principles of frontier orbital theory. The theory posits that reactivity is influenced by how well the energies of reactant frontier orbitals match energetically and spatially. Moreover, the energies of these one-electron orbitals can be modified, not directly by a field itself but by altering the electrostatic potential of the reactants.

First order perturbation theory is useful in making this concept more concrete. The first order correction to the energy of the ith molecular orbital, ϕ_i, due to an electrostatic potential, $V_e(r)$, is,

$$E_i^{(1)} = \langle \phi_i | V_e(r) | \phi_i \rangle \tag{1}$$

This correction depends only on the potential. The electric field enters the correction to the

3

extent that it alters the potential. In the case of a uniform z oriented EEF of strength F_z, an electron will see an electrostatic potential that increases with z. The electrostatic potential experienced by an electron in such a field is given as $V_e(z) = F_z \, q_e \, z$, where q_e is the electron charge and z is a coordinate relative to some arbitrary origin. Choice of a different origin gives different values for $V_e(z)$, but the difference between the potential at two points will be unaffected.

Using this form for the potential in equation 1, yields,

$$E_i^{(1)} = -F_z\langle\phi_i|z|\phi_i\rangle = -F_z \int z \, \rho_i \, dV \tag{2}$$

where $\rho_i = \langle\phi_i|\phi_i\rangle$ is the electron density of the ith MO and the integral is taken over all space. Note that this correction is independent of the polarity of ϕ_i—another indication that this third model for the action of an electric field on reactivity may be independent from the others.

We will demonstrate that this third model can be used to clearly rationalize computational findings simulating the influences of OEEFs on enzyme active sites, findings that have previously been challenging to interpret. This insight extends to understanding the mechanisms underlying the catalytic activity of natural enzymes, potentially aiding in the strategic use of electric fields to enhance or suppress chemical reactions.

Our problems of interest derive from quantum mechanical studies[19–22] exploring the effect of electric fields on high-valent iron-oxo heme proteins: e.g., catalases, peroxidases, and peroxygenases/monooxygenases.[23–26] Though there are hundreds of enzymes in these three classes, they share an active moiety referred to as Compound I (Cpd I) (Figure 1A), which varies only in the axial ligand coordinating the heme's iron center, with tyrosine, histidine, and cysteine in the catalases, peroxidases, and peroxygenases/monooxygenases, respectively.

Significant property variations are observed within each of these enzyme classes. It is well established that these variations are due to the axial ligand.[27] Recently, however, it was realized that equally important for reactivity control are the electric fields exerted on
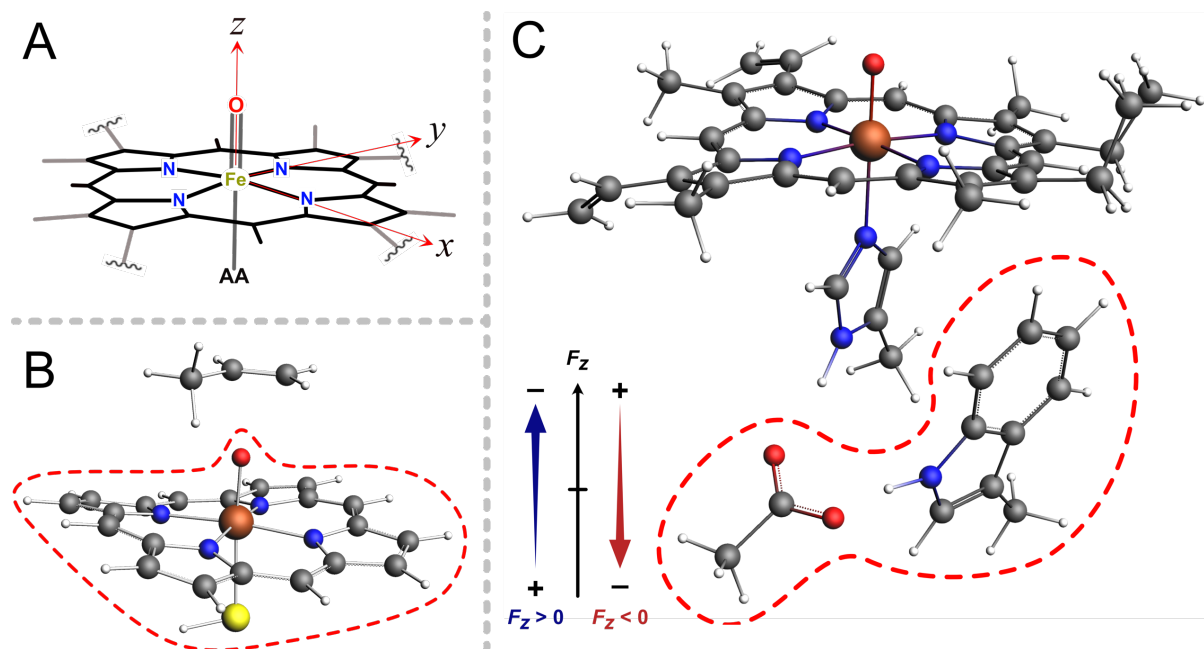
4

Figure 1: QM systems considered in this study. A) Compound I: the active moiety common to catalases, peroxidases, and peroxygenases/monooxygenases. The variants of these enzymes differ in their extended structure and in the axial amino acid (AA) residue: His, Cys, or Tyr. Active site model of Cys-ligated heme enzymes (B; heme fragment in red dashed region) and His-ligated heme enzymes (C). The (red dashed line) circled atoms designate the Trp-fragment and the others as the heme-fragment. The field direction is aligned with the Fe–O internuclear axis with the positive direction pointing from Fe to O. Atomic coordinates for these clusters are reported in the SI.

5

Cpd I by the enzyme's extended structure (excluding the heme and the axial ligand).[19] Bím et al. examined electric fields experienced by the Fe center in Cpd I in approximately 200 individual iron-oxo heme proteins and found that for all these proteins, the component of the electric field normal to the heme plane, F_z, was dominant. Furthermore, for His-ligated enzymes a strong negative (pointing from the axial oxygen ligand to the iron) F_z was observed most often while for Cys-ligated enzymes this field was exclusively positive (pointing from the iron to the axial oxygen ligand), with an average value of 28.5 MV/cm ($\sim$0.005 au). In Tyr-ligated catalases, the fields were uniformly near zero.

As another step toward rationalizing the effects of these fields on properties, researchers performed first-principles calculations on active site analogues (Figure 1B) subject to an OEEF mimicking the electric field from the remainder of the enzyme's extended structure.[19–21] These calculations resulted in two confounding observations.

The first of these concerned the effect of an OEEF on the unpaired electrons of His-ligated Cpd I—typically a triradicaloid species with three unpaired electrons.[21] Of these, in model systems, two occupy orthogonal π^* antibonding orbitals of the Fe-O functionality and the third is located on the heme's porphyrin ring, except for His-ligated Cpd I subject to a negative OEEF. Under this condition, the third unpaired electron is displaced to neighboring amino acid residues. How a field merely pointing from O to Fe in Cpd I can cause such dramatic changes in the electronic structure remains unexplained.[19]

The second observation concerns Cys-ligated heme proteins, some of which have the remarkable ability to catalyze both electrophilic epoxidation and nucleophilic hydroxylation. Shaik et al.,[22] using small molecule models of Cys-ligated Cpd I, revealed that the selectivity between epoxidation and hydroxylation could be switched by altering the direction and magnitude of F_z. With positive values favoring epoxidation and negative values favoring hydroxylation. The authors noted that they could provide no straightforward explanation for these results but speculated that the effects originated from field induced state mixing.

Given the key role of heme-Fe proteins in nature, understanding their function remains

6

an important frontier in biochemistry. It is highly desirable to have a model for the effect of electric fields that accounts for all observations, and thus has predictive power, for example in enzyme design. In this work, we show that Model 3, linking orbital behavior to electrostatic potential, satisfies this requirement, and therefore promises to be instrumental in describing and manipulating enzyme electrostatics.

Computational Methods

We reprised the above calculations using the same active site analogues as those employed in references 17 and 24 and shown in Figure 1B and C. For these calculations we used the Amsterdam Density Functional (ADF) package.[28,29] For a subset of these, we compared results using the B3LYP hybrid functional[30] with those using the less computationally demanding GGA-PBE functional.[31] The results varied only slightly, while agreeing qualitatively with calculations of other researchers.[19,22] And for the broad explanations given here, the various functionals employed led to the same conclusions. Hence, the full set of calculations reviewed here employed the GGA-PBE functional and a triple zeta with polarization Slater-type-orbital basis set.

In addition, we took advantage of ADF's fragment orbital capability in which molecular orbitals are expanded as a linear combination of the orbitals of predefined molecular fragments, so called fragment orbitals (FOs). Presenting the results in the form of fragment correlation diagrams provides the ideal visual tool to assess the effects of varying electrostatic potential on the electronic structures of the Cpd I analogues.

His-ligated peroxidases

The His-ligated peroxidases, for example, cytochrome c peroxidase (CcP), Leishmania major peroxidase (LmP), and ascorbate peroxidase (APX), are virtually homologous about the heme iron. In addition to their His-ligation, they share adjacent Trp and Asp residues, which

7

together form a hydrogen bonded network that contributes to the enzyme's properties.[32] The active site of these enzymes has been modeled with an analogue system shown in Figure 1B and C, where the His-axial ligand is replaced with imidazole while acetic acid and indole replace the side chains of the neighboring Asp and Trp residues.[19,21]

It should be noted that though the active site analogues across this series of peroxidases are virtually invariant, the LEF at their iron sites change. For example, the static fields computed from crystal structure data give APX $F_z = 4$ MV/cm, while for LmP and CcP $F_z = -16$ and -27 MV/cm, respectively (the field direction convention is shown in Figure 1C).[19] This variation is the result of their differing extended structures and lends support to the hypothesis that the active site LEF, and hence extended structure, plays an important role in mediating enzyme properties.

To capture the variations in electronic structure due to the differing fields, a z directed OEEF was included in the active site model of Figure 1C.[19,21] As has been mentioned, for a positive F_z one of the radicals of this triradical species was located on the porphyrin ring, but for a negative F_z this radical is displaced to the adjacent Trp and Asp residues. The ultimate factor differentiating between these two radicals awaits clarification.[19]

We performed three DFT fragment calculations on the His-ligated active site model of Figure 1C with an electric field of -0.01, 0, and $+0.01$ au (-51.4, 0, and 51.4 MV/cm) applied along the z-direction. These calculations employed two fragments, as designated in Figure 1C: a His-coordinated heme, referred to as the heme-fragment, and the analogues for the Trp and Asp residues, referenced as the Trp-fragment. Partial correlation diagrams representing the principal interactions between fragment orbitals (FOs) to produce the frontier region active site cluster MOs are shown in Figure 2. More detailed correlation diagrams are provided as Figures S1, S2, and S3 in the SI.[a]

The obvious effect of the OEEF is to change the relative energies of the fragment orbitals as per Equation 2. Compared to the zero field, the negative field shifts the Trp-fragment

---

[a]We used both the doublet and the quartet configurations for the full Trp-heme complex with no substantive difference to the correlation diagrams. The results shown here are for the quartet configuration.
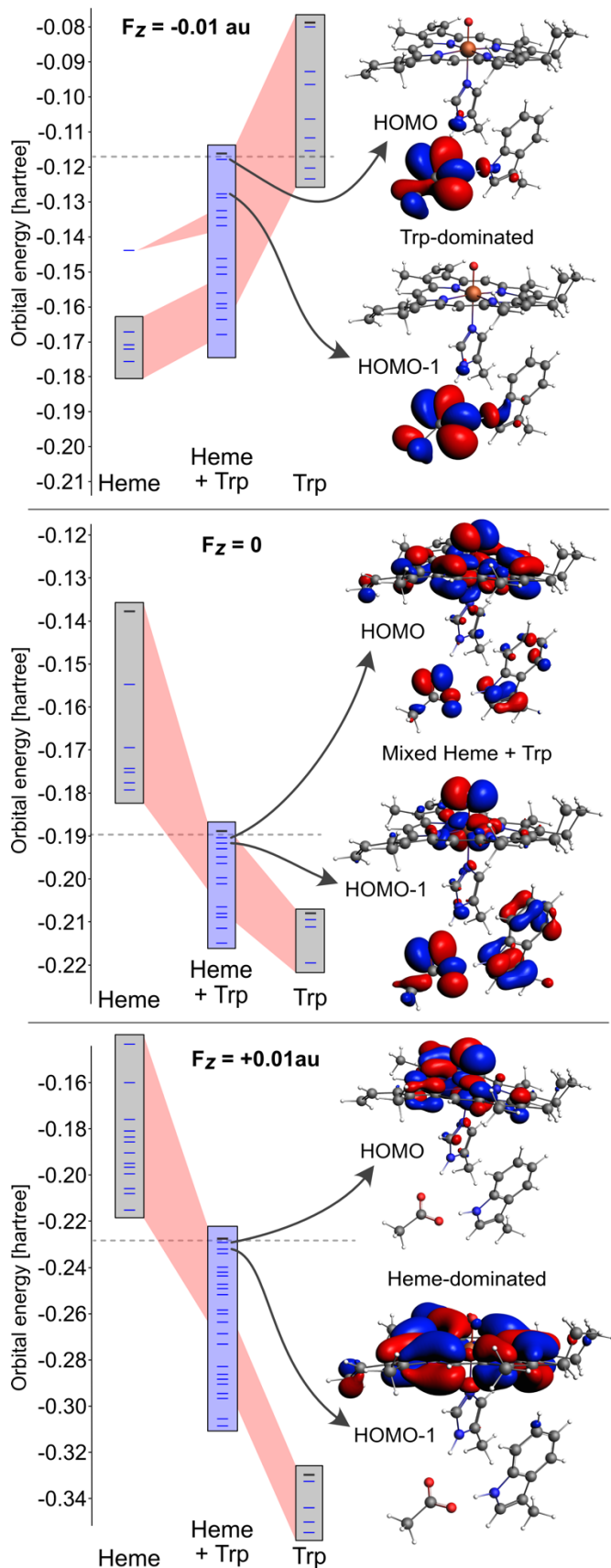
8

Figure 2: Partial correlation diagrams illustrating key interactions between the Trp-fragment and His-ligated heme-fragment frontier regions under a static external electric field of −0.01, 0, and +0.01 au (from top to bottom), and the corresponding HOMO and HOMO-1 orbital manifolds. The heme-fragment's occupied frontier orbitals create a π-complex involving S, Fe, and O atoms. The Trp-fragment's frontier orbitals consist of the π orbitals from the acetic acid and indole complex. Observe the notable shifts in orbital energy levels between the heme and Trp fragments under the influence of the electric field, leading to changes in the active site's frontier orbital character. At a zero field (center image), these fragment orbitals mix equally, forming the Trp-heme complex's occupied frontier orbitals. A negative field (top image) reduces the energy levels of the heme-fragment orbitals, preventing their mixing with the Trp-fragment's occupied frontier orbitals. Conversely, a positive field (bottom image) results in the opposite effect. The dotted line represents the estimated midpoint energy of the HOMO/LUMO gap in the Trp-heme complex.

9

FOs significantly up in energy relative to the heme-fragment FOs, while the positive field has the opposite effect.

The effect of these energy shifts is evident in the character of the frontier orbitals of the full heme-Trp complex. Shown in Figure 2 are the HOMO and HOMO-1 for each of the three applied electric fields. As is evident, for the negative field, shifting the energies of the Trp FOs up in energy leads to poor energy overlap between the frontier orbitals of the Trp- and heme-fragments, hence the frontier orbitals of the active site cluster are now Trp-like. The opposite response is seen for the positive field. Accordingly, under the influence of a positive field the unpaired electron will be in heme-orbitals and under the influence of a negative field in Trp-orbitals.

Cytochrome P450

We turn now to the remarkable demonstration that the selectivity between competing propene epoxidation and hydroxylation pathways could be switched by altering the direction and magnitude of an OEEF.[22] Using a small molecule model system representing the Cys-ligated Cpd I of cytochrome P450 (Figure 1B), Shaik et al. calculated that an OEEF with $F_z = \pm 0.01$ au would realize a 100% selectivity toward nucleophilic C–H or electrophilic C=C bond activation.[22]

In their investigation, Shaik et al. used DFT methods to calculate the reaction path and transition state energies for both propene hydroxylation and epoxidation as catalyzed by the analogue of Cys-ligated Cpd I of Figure 1B. The rate-limiting step in each process was determined to be the activation of either the C–H or C=C bond by the oxo-group of Cpd I, resulting in the formation of an alcohol or an epoxide, respectively.

In the absence of a field, the calculated transition state for epoxidation was found to be nearly degenerate with that for hydroxylation. However, for a uniform OEEF with $F_z = 0.01$ au the transition state for C–H bond activation (hydroxylation) was calculated to be 6-10

10

kcal/mol lower than that for C=C bond activation (epoxidation), while for $F_z = -0.01$ au the epoxidation process was calculated to be preferred by 2-6 kcal/mol.

To explain these observations, Shaik et al. investigated OEEF induced changes to the spin and charge densities of their active site model. They found that in the presence of an electric field oriented in the positive z-direction, the third unpaired electron of Cpd I is located almost entirely on the Cys sulfur atom. When the field is reversed, most of the spin density is located on the porphyrin ring. These changes were accompanied by the transfer of about 0.3 electrons from the sulfur to the porphyrin for a positive field and the opposite for a negative applied field. Still, Shaik et al. offered no explanation for the mechanism through which these field-induced shifts to the charge density to alter the transition state energies for hydroxylation versus epoxidation; they speculated that the effects originated from field induced state mixing.

We performed fragment calculations on a propene-Cpd I analogue shown in Figure 1B, with the propene molecule serving as one fragment and the Cpd I analogue, referred to as the heme-fragment, as the other. Partial correlation diagrams of the near frontier orbitals for an OEEF of −0.01, 0, and +0.01 au are shown in Figure 3. (More detailed correlation diagrams are provided at Figures S4, S5, and S6 in the SI.) The HOMO and LUMO of the propene-fragment are respectively the π bonding and antibonding orbitals of the propene double bond. These FOs will shift down in energy relative to the FOs of the heme-fragment when $F_z < 0$ and up when $F_z > 0$. These shifts affect the character of the frontier orbitals of the heme-propene complex.

For $F_z > 0$, the propene HOMO is well matched energetically with the HOMO of the heme-fragment ($\Delta E = 0.031 E_{\mathrm{h}}$), promoting strong overlap. However, propene's π^* antibonding LUMO is energetically distant from the heme-fragment's frontier orbitals ($\Delta E = 0.233 E_{rmh}$, note the discontinuities along the energy axis of Figure 3), preventing any mixing of these states. Conversely, an F_z of −0.01 au substantially reduces the energy of propene's HOMO relative to the frontier orbitals of the heme fragment ($\Delta E = -0.116 E_{\mathrm{h}}$), thus reduc-
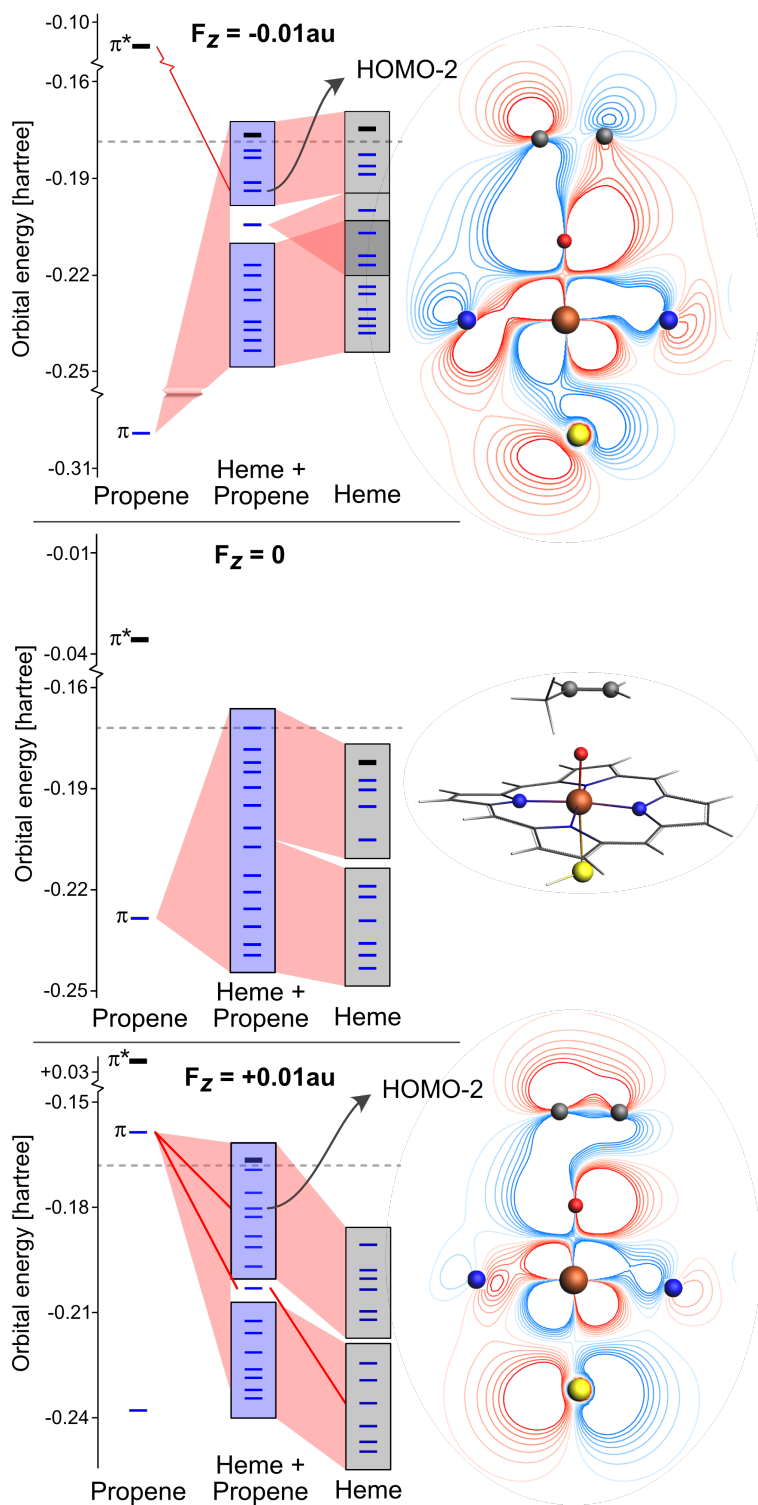
11

Figure 3: Partial correlation diagrams for the interactions between the frontier regions of the propene molecule and the Cys-ligated heme subjected to external electric field of (from top to bottom): -0.01, 0.00, and $+0.01$ au, along with contours of the corresponding spin majority HOMO-2 in the XZ plane. Note the discontinuities along the energy axes. The energies between the HOMO of the heme fragment and the π^* antibonding orbital of propene are 0.075, 0.151, and 0.223 E_h for fields of -0.01, 0, and $+0.01$ au respectively, while the energies between the HOMO of the heme fragment and propene's π^* antibonding orbital are 0.075, 0.151, and 0.223 E_h for fields of -0.01, 0, and $+0.01$ au respectively. In the presence of the negative field, the spin-majority HOMO-2 shows propene π^* antibonding character, while for the positive field, it is characterized by π bonding character.

ing their overlap. Simultaneously, it decreases the relative energy of propene's π^* antibonding orbital ($\Delta E = 0.075 E_h$) enough to allow it to interact with the heme-fragment's frontier orbitals. These effects are illustrated in Figure 3 with contour plots of the majority spin orbital just below the HOMO of the propene-heme complex. The negative field has introduced electron density into the π^* antibonding orbital of propene. Such electron redistribution is consistent with the Dewar-Chatt-Duncanson model[33] for C=C bond activation, offering a mechanism for epoxide formation through the application of a negative OEEF.
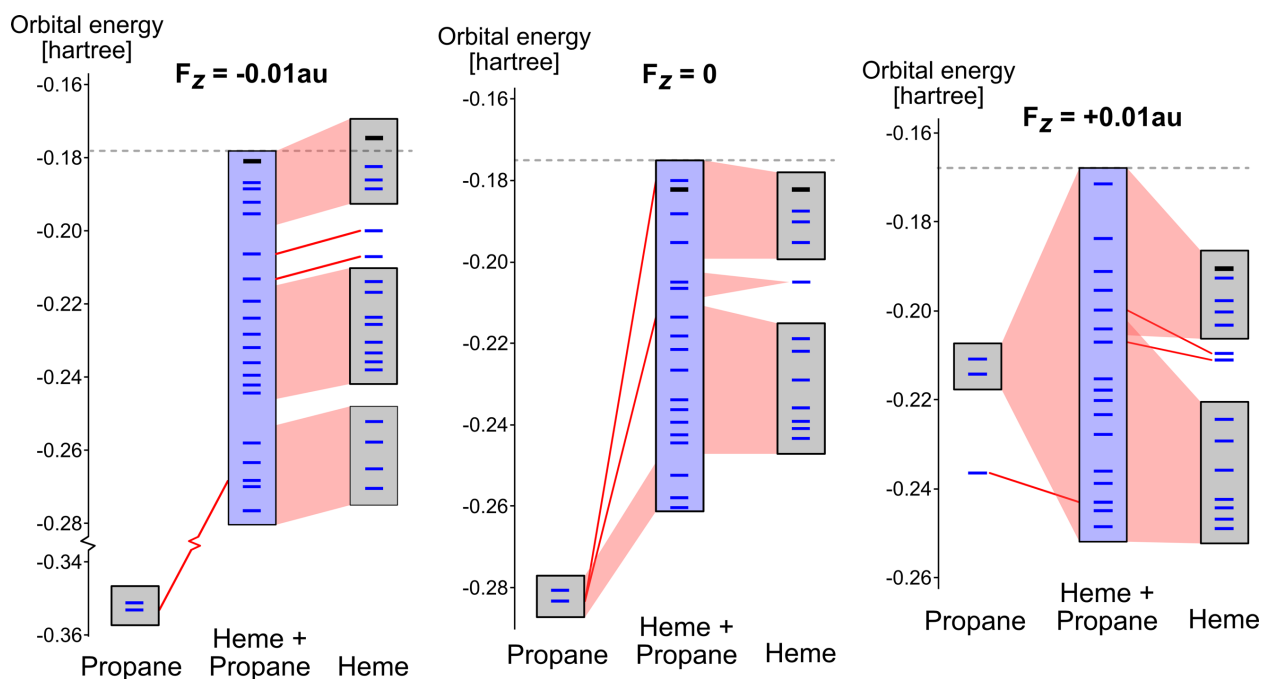

Figure 4: Frontier molecular orbitals displaying the propane Cys-ligated heme interaction due to an applied field. The negative field depresses the energy of the occupied propane FOs to such an extent that there is little to no overlap with the heme frontier orbitals (left). With the positive field, the propane FOs are raised in energy and now mix with the heme FOs (right). The dotted line indicates the approximate energy at the HOMO/LUMO midpoint of the propene-heme complex.

To better explore how a positive field facilitates C–H bond activation, we substituted the propene molecule (C–H bond dissociation energy (BDE) $\sim$85 kcal/mole) in Figure 1B with propane (BDE $\sim$100 kcal/mole) and conducted three fragment calculations with OEEFs of -0.01, 0, and $+0.01$ au. The corresponding partial correlation diagrams are shown in Figure 4. (Detailed correlation diagrams are shown as figures S7, S8, and S9 in the SI.)

13

Of note are the energies of the nearly degenerate propane-fragment H–C σ bonding HOMO and HOMO-1. In the absence of an OEEF (center pane Figure 4) these orbitals are located well below the frontier orbitals of the heme-fragment, occasioning little propane contribution to the reactive complex's frontier orbitals. The situation is exasperated in the presence of a negative field (left pane Figure 4) where propane's HOMO is so far removed from the heme-fragment frontier orbitals as to make mixing between the two negligible. However, a positive field (right pane Figure 4) brings the energy of propane's HOMO and HOMO-1 into near alignment with the heme-fragment frontier orbitals and yields the frontier orbitals of the reactive complex to be of mixed propane-heme character. Because the z-coordinate of the heme fragment is approximately 0, it is less responsive to the OEEF than those of propane with $F_z > 0$.

Scheme 1: The catalyzed reaction.

We investigated the effects of this enhanced mixing by calculating the electronic structure and molecular orbital manifold along a reaction profile transferring a hydrogen atom from propane to the oxo-ligand of Cpd I to form what is known as compound II (Cpd II) and a C3H7 radical (Scheme 1)—the first step in the overall hydroxylation reaction.

Because the cytochrome P450 active site model shown in Figure 1C does not include a substrate pocket, our calculation is a poor representation of the reaction dynamics of the enzyme. However, our purpose was to compare the relative stabilities of the fragment configurations along the reaction profile in the presence of positive and negative applied fields.

Figure 5 shows the calculated reaction profile for an applied field of +0.01 au A TS with an energy of $\sim$ 4 kcal/mole was found approximately 40% of the way along the reaction coordinate. Early in the reaction the heme-propane HOMO-1 results from mixing propane's
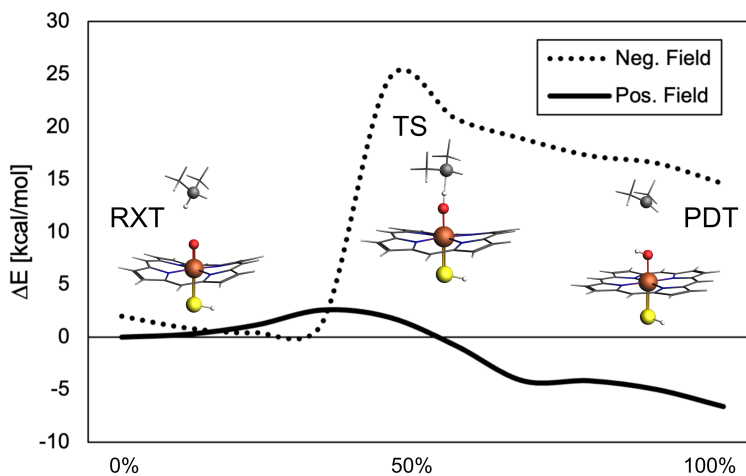
14

Figure 5: The reaction profile in the presence of the +0.01 au applied field is shown (solid), as well as the corresponding profile of the same reaction path but with a −0.01 au field applied. The reactant, transition state, and product states are depicted, with important atoms emphasized. See SI for more detail.

HOMO with the heme-fragment's LUMO. Later, the mixing between occupied propane FOs and unoccupied heme FOs become more intense. Where the heme-propane HOMO and HOMO-1 derive from mixing between propane's HOMO and unoccupied heme FOs. This mixing is made possible by the field induced near degeneracy of the propane and heme-fragment frontier orbitals. A situation that is intensified through the course of the reaction because propane's HOMO increases its energy as the H–C σ bonding interaction grows weaker. Thus, through the reaction, the energy of propane's HOMO matches increasingly well with the unoccupied heme-fragment orbitals, leading to greater overlap between propane and enzyme frontier orbitals.

Also shown in Figure 5 is the energy along the same reaction path with an applied field of −0.01 au. This path is strongly field destabilized with a maximum along the path of ~ 25 kcal/mole and a positive ΔH_{rxn}. However, the configuration at this point does not represent a true TS as the negative field alters the potential energy surface. A negative field TS calculation with the same initial and final states as in Figure 5 recovers a reaction path profile qualitatively like the dotted path shown in Figure 5 but with a distinct TS configuration with an energy of ~ 13 kcal/mole and again a positive ΔH_{rxn}. Inspection

15

of the frontier MOs of the propane-heme complex show no contribution from the propane fragment orbitals, consistent with Figure 4.

Clearly, the negative field lowers the energy of propane's frontier orbitals to such an extent that mixing with the unoccupied heme-fragment orbitals is not favored. Instead, propane's occupied frontier orbitals mix with occupied orbitals of the heme-fragment, minimizing the charge transfer from propane to the heme-fragment. In fact, the negative field lowers the energy of propane's unoccupied FOs sufficiently to produce a small amount of mixing with the occupied heme-fragment orbitals. This mixing, though small, leads to charge transfer from the heme-fragment to propane. The reverse direction of what is observed in the catalytic process of Scheme 1.

As a final observation, HOMO-LUMO energy gaps have been associated with chemical hardness,[34] where a smaller energy gap indicates greater chemical reactivity and decreased kinetic stability. If one takes the energy difference between the orbitals involved in charge transfer, e.g., propane's HOMO and the heme-fragment's LUMO, as the HOMO-LUMO energy gap for this reaction, then the application of a positive field softens the reaction and a negative field act to harden it.

Summary

We introduce a physical model that attributes puzzling effects of electric fields on heme-Fe reactivity to shifts in the energy levels of reactant fragment orbitals (such as heme, Trp, and reaction substrate) due to changes in electrostatic potential induced by the fields. These energy shifts depend solely on the local electrostatic potential and are not influenced by orbital characteristics. These shifts modify the interaction of frontier orbitals, thus enhancing or reducing reactivity. We demonstrate that significant changes in the electronic structure of His-ligated Cpd I under electric fields can be explained by the energy shifts of fragment orbitals on the Fe-heme complex and an adjacent Trp residue. Additionally, we illustrate how

16

the selectivity between epoxidation and hydroxylation in Cys-ligated Cpd I is influenced by field-induced variations in the energy of fragment orbitals from the Cys-ligated Fe-heme and the reacting substrate. Further, we hypothesize that the energy difference between fragment orbitals involved in inter-fragment charge transfer may quantitatively evaluate the impact of electric fields on reactivity and selectivity.

This analysis offers an additional perspective from which to analyze the effects due to electrostatic preorganization and to predict how these effects may alter an enzyme's reactivity. We hope that this perspective will be broadly applicable, aside from the Fe-heme chemistry used here as a model system. This opens a path to field engineering via sequence mutagenesis, with the orbital alignment as the goal, toward desired reactivity. Alternatively, one can think of modifying the substrate, the co-factor, or the nearby amino acids to non-natural ones, which would produce the desired alignments and induce reactivity new to nature.

Acknowledgments

References

(1) Pocker, Y.; Buchholz, R. F. Electrostatic Catalysis of Ionic Aggregates. I. Ionization and Dissociation of Trityl Chloride and Hydrogen Chloride in Lithium Perchlorate-Diethyl Ether Solutions. *Journal of the American Chemical Society* **1970**, *92*, 2075–2084.

(2) Aragonès, A. C.; Haworth, N. L.; Darwish, N.; Ciampi, S.; Bloomfield, N. J.; Wallace, G. G.; Diez-Perez, I.; Coote, M. L. Electrostatic Catalysis of a Diels–Alder Reaction. *Nature* **2016**, *531*, 88–91.

(3) Kim, W. Y.; Kim, K. S. Tuning Molecular Orbitals in Molecular Electronics and Spintronics. *Accounts of Chemical Research* **2010**, *43*, 111–120.

(4) Shaik, S.; Mandal, D.; Ramanan, R. Oriented Electric Fields as Future Smart Reagents in Chemistry. *Nature Chemistry* **2016**, *8*, 1091–1098.

17

(5) Shaik, S.; Ramanan, R.; Danovich, D.; Mandal, D. Structure and Reactivity/Selectivity Control by Oriented-External Electric Fields. *Chemical Society Reviews* **2018**, *47*, 5125–5145.

(6) Ciampi, S.; Darwish, N.; Aitken, H. M.; Díez-Pérez, I.; Coote, M. L. Harnessing Electrostatic Catalysis in Single Molecule, Electrochemical and Chemical Systems: A Rapidly Growing Experimental Tool Box. *Chemical Society Reviews* **2018**, *47*, 5146–5164.

(7) Thayer, A. M. Drug Repurposing. *Chemical & Engineering News* **2012**, *90*.

(8) Ro, D.-K.; Paradise, E. M.; Ouellet, M.; Fisher, K. J.; Newman, K. L.; Ndungu, J. M.; Ho, K. A.; Eachus, R. A.; Ham, T. S.; Kirby, J.; Chang, M. C. Y.; Withers, S. T.; Shiba, Y.; Sarpong, R.; Keasling, J. D. Production of the Antimalarial Drug Precursor Artemisinic Acid in Engineered Yeast. *Nature* **2006**, *440*, 940–943.

(9) Stuyver, T.; Danovich, D.; Joy, J.; Shaik, S. External Electric Field Effects on Chemical Structure and Reactivity. *WIREs Computational Molecular Science* **2020**, *10*, e1438.

(10) Zheng, C.; Mao, Y.; Kozuch, J.; Atsango, A. O.; Ji, Z.; Markland, T. E.; Boxer, S. G. A Two-Directional Vibrational Probe Reveals Different Electric Field Orientations in Solution and an Enzyme Active Site. *Nature Chemistry* **2022**, *14*, 891–897.

(11) Zhao, X.; Liu, M.; Wang, Y.; Xiong, Y.; Yang, P.; Qin, J.; Xiong, X.; Lei, Y. Designing a Built-In Electric Field for Efficient Energy Electrocatalysis. *ACS Nano* **2022**, *16*, 19959–19979.

(12) Siddiqui, S. A.; Stuyver, T.; Shaik, S.; Dubey, K. D. Designed Local Electric Fields-Promising Tools for Enzyme Engineering. *JACS Au* **2023**, *3*, 3259–3269.

(13) Weberg, A. B.; Murphy, R. P.; Tomson, N. C. Oriented Internal Electrostatic Fields: An Emerging Design Element in Coordination Chemistry and Catalysis. *Chemical Science* **2022**, *13*, 5432–5446.

(14) Welborn, V. V.; Ruiz Pestana, L.; Head-Gordon, T. Computational Optimization of Electric Fields for Better Catalysis Design. *Nature Catalysis* **2018**, *1*, 649–655.

(15) Warshel, A. Electrostatic Origin of the Catalytic Power of Enzymes and the Role of Preorganized Active Sites. *The Journal of Biological Chemistry* **1998**, *273*, 27035–27038.

(16) Warshel, A.; Sharma, P. K.; Kato, M.; Xiang, Y.; Liu, H.; Olsson, M. H. M. Electrostatic Basis for Enzyme Catalysis. *Chemical Reviews* **2006**, *106*, 3210–3235.

(17) Warshel, A.; Weiss, R. M. An Empirical Valence Bond Approach for Comparing Reactions in Solutions and in Enzymes. *Journal of the American Chemical Society* **1980**, *102*, 6218–6226.

18

(18) Wasileski, S. A.; Koper, M. T. M.; Weaver, M. J. Field-Dependent Electrode-Chemisorbate Bonding: Sensitivity of Vibrational Stark Effect and Binding Energetics to Nature of Surface Coordination. *Journal of the American Chemical Society* **2002**, *124*, 2796–2805.

(19) Bím, D.; Alexandrova, A. N. Local Electric Fields As a Natural Switch of Heme-Iron Protein Reactivity. *ACS Catalysis* **2021**, *11*, 6534–6546.

(20) de Visser, S. P. What External Perturbations Influence the Electronic Properties of Catalase Compound I? *Inorganic Chemistry* **2006**, *45*, 9551–9557.

(21) de Visser, S. P. What Affects the Quartet-Doublet Energy Splitting in Peroxidase Enzymes? *The Journal of Physical Chemistry A* **2005**, *109*, 11050–11057.

(22) Shaik, S.; de Visser, S. P.; Kumar, D. External Electric Field Will Control the Selectivity of Enzymatic-Like Bond Activations. *Journal of the American Chemical Society* **2004**, *126*, 11746–11749.

(23) Huang, X.; Groves, J. T. Oxygen Activation and Radical Transformations in Heme Proteins and Metalloporphyrins. *Chemical Reviews* **2018**, *118*, 2491–2553.

(24) Moody, P. C. E.; Raven, E. L. The Nature and Reactivity of Ferryl Heme in Compounds I and II. *Accounts of Chemical Research* **2018**, *51*, 427–435.

(25) Poulos, T. L. Heme Enzyme Structure and Function. *Chemical Reviews* **2014**, *114*, 3919–3962.

(26) Sono, M.; Roach, M. P.; Coulter, E. D.; Dawson, J. H. Heme-Containing Oxygenases. *Chemical Reviews* **1996**, *96*, 2841–2888.

(27) Balcells, D.; Raynaud, C.; Crabtree, R. H.; Eisenstein, O. A Rational Basis for the Axial Ligand Effect in C-H Oxidation by [MnO(Porphyrin)(X)]+ (X = H2O, OH-, O2-) from a DFT Study. *Inorganic Chemistry* **2008**, *47*, 10090–10099.

(28) te Velde, G.; Bickelhaupt, F. M.; Baerends, E. J.; Fonseca Guerra, C.; van Gisbergen, S. J. A.; Snijders, J. G.; Ziegler, T. Chemistry with ADF. *Journal of Computational Chemistry* **2001**, *22*, 931–967.

(29) Fonseca Guerra, C.; Snijders, J. G.; te Velde, G.; Baerends, E. J. Towards an Order-N DFT Method. *Theoretical Chemistry Accounts* **1998**, *99*, 391–403.

(30) Stephens, P. J.; Devlin, F. J.; Chabalowski, C. F.; Frisch, M. J. Ab Initio Calculation of Vibrational Absorption and Circular Dichroism Spectra Using Density Functional Force Fields. *The Journal of Physical Chemistry* **1994**, *98*, 11623–11627.

(31) Perdew, J. P.; Burke, K.; Ernzerhof, M. Generalized Gradient Approximation Made Simple. *Physical Review Letters* **1996**, *77*, 3865–3868.

19

(32) Goodin, D. B.; McRee, D. E. The Asp-His-iron Triad of Cytochrome c Peroxidase Controls the Reduction Potential Electronic Structure, and Coupling of the Tryptophan Free Radical to the Heme. *Biochemistry* **1993**, *32*, 3313–3324.

(33) Chatt, J.; Duncanson, L. A.; Venanzi, L. M. Directing Effects in Inorganic Substitution Reactions. Part I. A Hypothesis to Explain the Trans-Effect. *Journal of the Chemical Society (Resumed)* **1955**, 4456–4460.

(34) Pearson, R. G. Hard and Soft Acids and Bases—the Evolution of a Chemical Concept. *Coordination Chemistry Reviews* **1990**, *100*, 403–425.